IEEE Photonics Journal
An IEEE Photonics Society Publication

Open Access

Experimental Measurement of Fiber-Wireless Transmission via Multimode-Locked Solitons From a Ring Laser EDF Cavity

Volume 7, Number 2, April 2015

I. S. Amiri
S. E. Alavi
M. R. K. Soltanian
H. Ahmad
N. Fisal
A. S. M. Supa'at

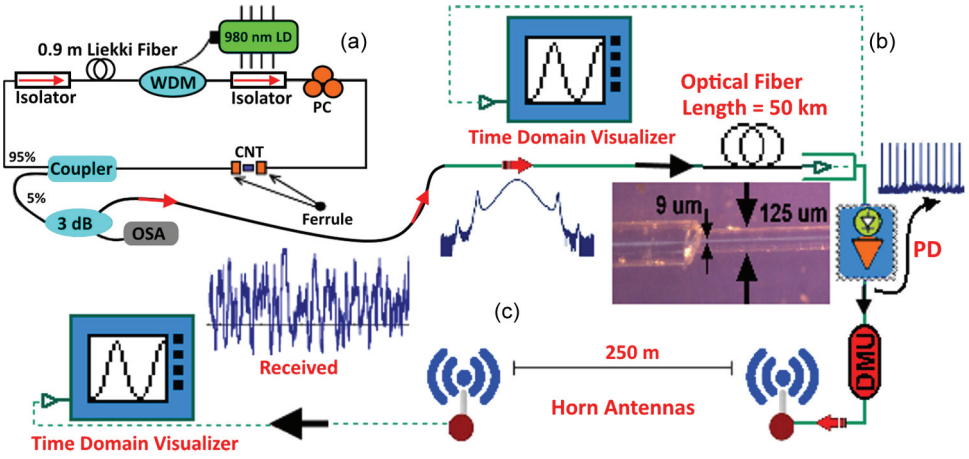

DOI: 10.1109/JPHOT.2015.2408438
1943-0655

IEEE photonics SOCIETY

IEEE

Experimental Measurement of Fiber-Wireless Transmission via Multimode-Locked Solitons From a Ring Laser EDF Cavity

I. S. Amiri,[1] S. E. Alavi,[2] M. R. K. Soltanian,[1] H. Ahmad,[1] N. Fisal,[2] and A. S. M. Supa'at[3]

[1]Photonics Research Centre, University of Malaya, 50603 Kuala Lumpur, Malaysia
[2]UTM MIMOS CoE in Telecommunication Technology, Faculty of Electrical Engineering, Universiti Teknologi Malaysia, 81310 Skudai, Malaysia
[3]Lightwave Communication Research Group, Faculty of Electrical Engineering, Universiti Teknologi Malaysia, 81310 Skudai, Malaysia

DOI: 10.1109/JPHOT.2015.2408438

Manuscript received February 13, 2015; revised February 25, 2015; accepted February 25, 2015. Date of publication March 3, 2015; date of current version March 13, 2015. This work was supported by the Universiti Teknologi Malaysia PAS under Grant Q.J130000.2709.01K14. The work of I. S. Amiri and H. Ahmad was supported by the University of Malaya/MOHE under Grant UM.C/625/1/HIR/MOHE/SCI/29 and Grant RU002/2013. Corresponding author: S. E. Alavi (e-mail: sayedehsan@utm.my).

Abstract: This paper describes a demonstration of soliton transmission over fiber-wireless (Fi-Wi) networks using mode-locked stable solitons over a 50-km-long fiber and a short-distance wireless link. Ultrashort optical pulse sources in the 1.5-μm region are seen as increasingly important for achieving ultrahigh-speed optical transmission and signal processing at optical nodes. Mode-locked solitons were generated by a simple ring laser cavity incorporating a very thin layer of carbon nanotube (CNT), together with an erbium-doped fiber (EDF) laser used as an active bulk gain medium. Experimental measurements involved the transmission of the generated mode-locked soliton over a 50-km-long single-mode fiber (SMF), and a radio-frequency (RF) spectrum subsequently generated was a result of beating frequency of wavelengths launched into the photodetector at the other end of the SMF. This RF spectrum array was in the range of WiFi frequencies. System performance was evaluated by first selecting one of the RF carriers centered at 2.5 GHz via an RF bandpass filter and subsequently using this carrier to transmit quadrature phase-shift keying (QPSK) and 16-quadrature amplitude modulation (16-QAM) data signals. The described optical circuit, containing an EDF laser, a CNT, an SMF, and a wireless link, was shown to achieve ultrastable transmission of mode-locked soliton over a long-distance Fi-Wi network.

Index Terms: Multimode-locked soliton, Fiber-Wireless (Fi-Wi), ring laser EDF.

1. Introduction

Demands for expansion of high-speed communication systems have rendered ultrahigh-speed soliton light sources indispensable for the development of ultra-high speed optical time division multiplexing (OTDM) and ultra-high speed dense wavelength division multiplexing (DWDM) communications as a means to solve the capacity issue [1]–[3]. Transmission of soliton pulses via wired/wireless communication link has been presented in many publications by Amiri *et al.* in the

field of optical communications [4]–[12]. The generation of ultrashort pulses in the Gigahertz region is especially important in terms of realizing ultrahigh-speed OTDM transmission [13], [14]. Mode-locked fiber lasers have been shown as the most inexpensive optical light sources for practical generation of ultrashort pulses, with actively harmonic mode-locked erbium-doped fiber (EDF) lasers capable of producing transform-limited narrow Gaussian pulses with adjustable multi-GHz bit rates and variable pulsewidths in the picosecond range. Such systems are especially suitable for high speed, long distance WDM transmission [15]–[18]. A main application of the multiple soliton transmission system containing ring laser EDF cavities is high-data rate transmission for short and long distance communication. The unprecedented number of available signals in such devices provide for a potential much higher data rate compared to other bandwidth-limited channels that are used currently [19]–[21].

Mode-locked outputs are desired for ultra-fast pulses, although this comes at the cost of lessened pulse power. For true soliton mode-locking, soliton shaping effects play a dominant role and the pulse duration is nearly independent of other parameters [22], [23]. A saturable absorber (SA) is required for starting and stabilizing the mode-locking. The necessary limitation of nonlinear phase shifts, combined with the fundamental soliton condition, implies particular scaling laws for soliton mode-locked lasers. Fundamental soliton pulses are highly important in particular for long-distance optical fiber communications and in mode-locked lasers (soliton mode-locking) [24], [25]. In the latter situation, soliton-like pulses can be formed when the typically unavoidable factors of dispersion and nonlinearity in the laser cavity are negligible. Solitons are also applied in various techniques for pulse compression using optical fibers [26], [27]. An optical soliton pulse is the recommended foundation for the creation of a spectrum of light over a wide range [28], [29]. Optical solitons are powerful laser pulses that can be employed to generate multi-soliton filter characteristics [30].

This work is rationally intended to link and mash up the photonic generation of solitonic multicarriers concepts using mode-locked techniques with traditional wireless approaches. This paper details a study of the propagation of optical solitons within a nonlinear ring cavity and, specifically, a system of ring laser EDF cavities to generate mode-locked soliton used to form high capacity and secure transmittable signals applicable in optical communication. In this work, a successful transmission of ultra-stable soliton pulses over long distance optical links is described along with a subsequent generation of RF multicarriers in the WiFi spectrum range, from which the performance of RF carrier transmission over a 250 m wireless link is measured and analyzed. The proposed structural design described here can be used to generate and transmit a high density of optical soliton pulses over a fiber-wireless network.

A preferable system is the passively mode-locked fiber laser, since it is easier to operate and avoids the use of bulky active components which increase system complexity and cost. A passively mode-locked fiber laser can be realized by an interesting means involving incorporation of carbon nanotube (CNT) as a broadband SA within the laser cavity, and this addition allows for tunability over a wide wavelength range. Moreover, altering the cavity length provides an easy means of changing the RF free spectral range (FSR). A method is proposed for generating multiple carrier RF with very low phase noise, limited amplitude fluctuations, and identical time jitter along with negligible interference between carriers. The obtained results show that the proposed architecture is a promising scheme for the generation of multiple high purity carriers up to extremely high frequencies (W band) that are far beyond the reach of electronic oscillators [31].

2. Theoretical Background

Predictions regarding the formation and evolution of passively mode-locked laser pulses are frequently described by the master equation [32] and the complex Ginzburg-Landau equation [33], [34], which both provide exact solutions for solitons. The passive mode-locking feature of the laser system proposed in this paper is based on nonlinear polarization rotation evolution, whereby an ellipse is resolved into right- and left-hand circular polarization components of separate intensities. The two coupled nonlinear Schrodinger equations (NLSEs) that involve a vector electric

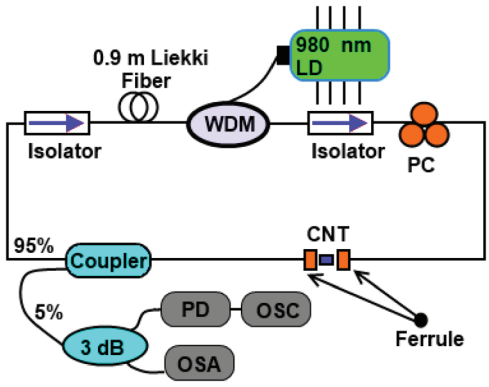

Fig. 1. Soliton mode-lock generation system setup, CNT stands for carbon nanotube, WDM for wavelength division multiplexing, PC for polarization controller, OSA for optical spectrum analyzer, PD for photodetector, and OSC for oscilloscope.

field are able to accurately model the light-wave propagation in the weakly birefringent fibers, although the coupled NLSEs must involve extra terms such as the wave-number difference between the two modes and the four-wave mixing when the total cavity is several meters in length [35]. Contrarily, the terms related to four-wave mixing can be ignored in the coupled equations if the total cavity length, L, exceeds 100 m, despite this length being far longer than the typical beat length, LB $\approx$ 1 m, of the fiber [36], [37]. The coupled-mode equations are expressed in [38].

The numerical simulations presented in the reference [38] show that, by appropriately setting the polarization of polarizer and analyzer and the linear cavity phase-delay bias of the cavity, self-started mode locking can be achieved. Since the saturation energy (E_s) is proportional to the pumping strength [39], increasing E_s corresponds to increase the pump power in the experiments.

3. Experimental Setup, Results, and Discussion

The experimental setup of the proposed soliton fiber laser is shown in Fig. 1. The laser used a 0.9 m long highly doped Leikki Er80-8/125 EDF as the active gain medium. The EDF was pumped backward by a Lumics 980 nm laser diode through a wavelength division multiplexer (WDM). One end of the EDF was connected to the common output of the WDM, while the other end was connected to an isolator to ensure no signals propagated in the opposite direction through the EDF. The isolator connected to the WDM was used to avoid any unwanted back reflection towards the gain medium. This isolator was in turn connected to a polarization controller (PC) and an embedded CNT between two ferrules. The output of the embedded CNT was guided toward a 95 : 5 coupler, which extracted a portion of the signal for analysis. The 95% port was connected to an isolator, which was then connected to the gain medium. This loop completed the laser cavity. The extracted output was divided into two evenly powered portions using a 3 dB coupler, with one portion being directed to an optical spectrum analyzer (OSA) (model YOKOGAWA AQ6370B, with wavelength resolution bandwidth accuracy of $\pm$ 0.02 nm (1520 to 1580 nm)) while the other portion led to a photodetector (HP lightwave detector DC-6 GHz) and finally to whether radio frequency-spectrum analyzer (RF-SA Anritsu MS2683A) or oscilloscope (YOKOGAWA DLM2054) in order to be analyzed separately to obtain the average output power, the radio frequency spectrum and the output in the time domain.

The all-fiber mode-locked soliton pulses generated via the CNT-based SA as a mode locker have their power across a wavelength range represented in Fig. 2(a). The total length of the laser cavity was approximately 4 m. Aside from the EDF, all fibers used in the cavity were Corning SMF-28 $(\beta_2 = -22\ \text{ps}^2/\text{km})$. The observed mode-locked pulses were achieved at a threshold pump power of about 40 mW, with the optical spectrum having a very wide-band output together with multiple sidebands present as observed in the OSA. The presence of these sidebands

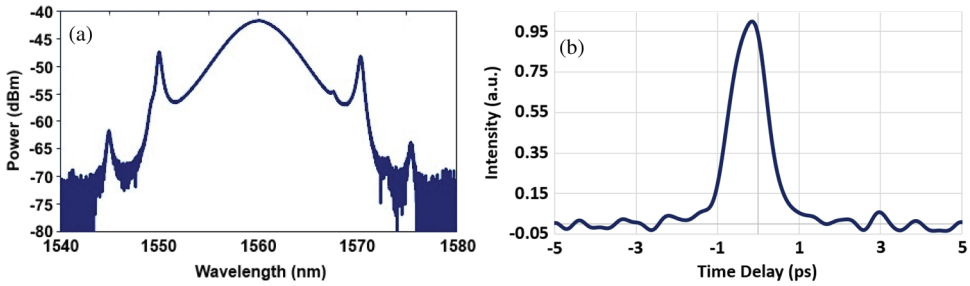

Fig. 2. (a) Mode-locked soliton generation and (b) the autocorrelation time delay of 670 fs.

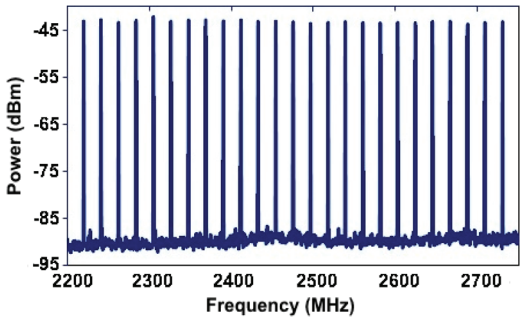

Fig. 3. Generated mode-locked solitons with FSR of 21.6 MHz and FWHM of 400 KHz in frequency domain in 550 MHz scale.

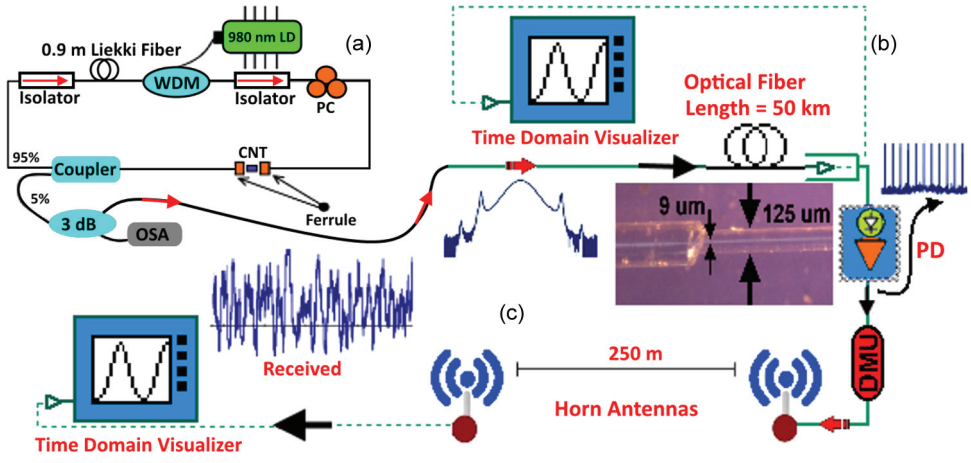

Fig. 4. Schematic of the Fi-Wi transmission setup, CNT stands for carbon nanotube, DMU for data modulator unit, WDM for wavelength division multiplexing, PC for polarization controller, and OSA for optical spectrum analyzer.

confirmed that the system was operating in the soliton regime. Fig. 2(b) provides the autocorrelation trace. The estimated pulse duration at the full-width at half maximum (FWHM) point was 670 fs with the assumption of a sech^2 pulse shape for the case of anomalous dispersion. Fig. 3 shows the beating frequency for each of the two modes available in the mode-locked soliton spectrum in 550 MHz scale.

The communication system based on RF signals generated from an optical soliton is shown in Fig. 4. This system involves three main parts:

a) multicarrier generator which is briefly discussed in Section 3;

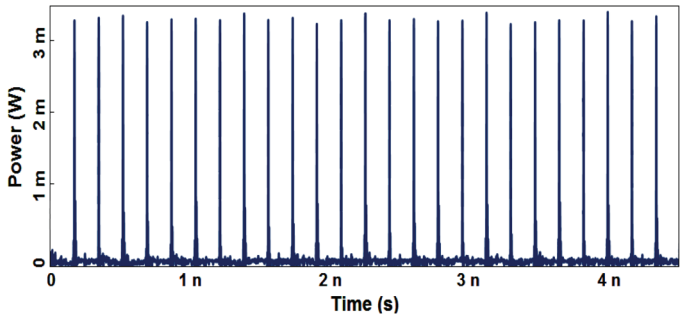

Fig. 5. Time-domain trace for the mode-locked soliton.

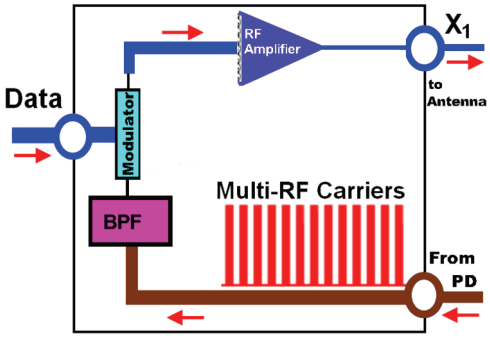

Fig. 6. Data modulator unit (DMU) used for modulating the generated RF carriers.

b) optical transmission line which is 50 km SMF link;
c) RF signal generation using DMU and wireless transmission using antennas.

In order to examine the stability of the generated mode locked soliton signal which is shown in Fig. 2(a), it was forwarded to 50 km optical fiber. This 50 km optical fiber had an attenuation of 0.2 dB/km, dispersion of 5 ps/(nm.km), differential group delay of 0.2 ps/km, nonlinear refractive index of 2.6×10^{-20} m^2/W, effective area of 25 μm^2 and nonlinear phase shift of 3 mrad. The size of the core and cladding of the single mode fiber was 9 and 125 μm respectively. The transmission of the mode locked soliton signal through 50 km of optical fiber can be seen in Fig. 5 in time domain which show the pulses with FWHM of 670 fs.

A PIN photodetector (PD) was used to convert the solitonic input power to RF band. An ideal rectangle filter was utilized to reduce the number of samples in the electrical signal generated from the incoming optical signal and noise bins. The generated RF spectrum was a result of beating frequency of wavelengths launched into the PD at the other end of the SMF After photo detection, at the data modulator unit (DMU), as shown in Fig. 6, the RF multicarriers are generated in the range of the WiFi frequency and can be modulated to transmit wirelessly along the 250 m wireless link. In order to check the performance of the whole system, one of the RF carriers centered at 2.5 GHz was selected using RF band pass filter (BPF), and this carrier was then used to transmit quadrature phase-shift keying (QPSK)/16-quadrature amplitude modulation (16-QAM) data signals. Following amplification, the modulated RF signal was forwarded to the transmitter antenna.

The center frequency can be defined or calculated automatically by centering the filter at the optical channel possessing maximum power. The power of the detected RF signal after transmission along a 50 km fiber link and within the 250 m wireless link distance can be seen in Fig. 7.

The FWHM of the pulse shown in Fig. 7 is 80 ps which is wider than the original one shown in Fig. 2(b) due to very long transmission medium.

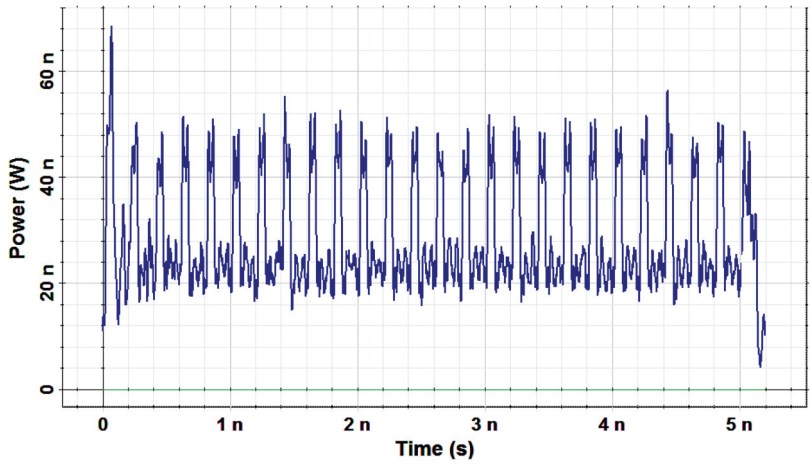

Fig. 7. Transmission of modulated 2.5GHz signals over a 250 m wireless link.

TABLE 1

Measured RF received power by changing the wireless distance

$d\ (m)$	0.20	12.0	22.0	32.0	42.0	52.0	62.0
$p_r(dBm)$	-1.10	-1.60	-2.20	-2.80	-3.40	-4.20	-4.90
$d\ (m)$	72.0	82.0	92.0	102.0	112.0	122.0	132.0
$p_r(dBm)$	-5.4	-9.5	-12.5	-14.8	-16.4	-18.2	-19.6
$d(m)$	142.0	152.0	162.0	172.0	182.0	192.0	202.0
$p_r(dBm)$	-20.7	-21.9	-23.1	-23.9	-24.6	-25.5	-26.2
$d(m)$	212.0	222.0	232.0	242.0	252.0		
$p_r(dBm)$	-27.4	-28.3	-29.2	-30.2	-32.1		

4. RF Power and EVM Measurement of the Wireless Transmission System

The radiometric parameters of the RF signal generated from soliton sources are not determined thus far in this paper. The radiated power of the solitonic-based RF signal transmission was measured via experiment, with the applied soliton pulses being those under discussion in Fig. 2 and the optical output solitonic power fixed to −10 dBm. An RF power meter was introduced to the experimental configuration and alignment assured by means of fixing the power meter appropriately. Distance between the antenna and power meter was increased from 0.2 m to 250 m at intervals of 10 m, and the received power was recorded at each interval. Table 1 shows the measured RF received power for each interval.

Observation of the measured data implies that −5 dBm optical power alters the radiated RF power from −1.10 to −32.10 dBm for the wireless distances from 0.2 to 252 m. However, it can be considered that a successful wireless transmission constitutes an average received power being the threshold power; which for this particular experiment was around −16 dBm and equivalent to almost a wireless distance of 120 meters. A further experiment had the wireless distance fixed to 120 meters and the optical power changed using a variable optical attenuator (VOA) in order to get the appropriate threshold for the minimum acceptable optical output power.

As can be seen from Table 2, the average received power was −24 dBm. This corresponded to −9.5 dBm optical power and determined the minimum threshold for optical power as −10 dBm. In the further experiment, the error vector magnitude (EVM) of the overall system was measured by fixing the optical power to −10 dBm and the wireless distance was changed from 0.2 to 120 meters. The EVM is used to quantify the modulation accuracy of a transmitter

TABLE 2

Measured RF received power with variation of optical power

Optical power (dBm)	-5	-6.5	-8	-9.5	-11	-12.5	-14
Measured RF power (dBm)	-18	-19.8	-22.1	-24.8	-26.2	-27.1	-30

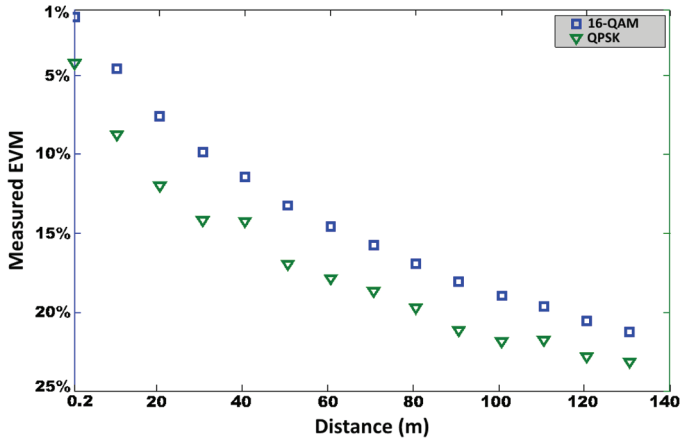

Fig. 8. Measured EVM of system based on wireless distance.

and constitutes a measure of the difference between a reference waveform, which is the error-free modulated signal, and the actual transmitted waveform. EVM. The EVM is defined as

$$\%\text{EVM} = 100 \times \left[\sum_{l=1}^{N} \frac{|d_r - d_l|}{N}\right]^{\frac{1}{2}} \Big/ d_{\max}$$

where d_r and d_l are the received and ideal symbol vectors, respectively, and $d_{\max}$ is the maximum symbol vector in the constellation, while N is the number of symbols [40]. According to [40], the EVM threshold for successful transmission is 5%, 7%, 10%, and 25% for 64-QAM, 32-QAM, 16-QAM, and QPSK modulation respectively. To estimate a bit error rate (BER) from EVM, L is defined as the number of identical signal levels within each dimension of the (quadratic) constellation, and Log_2^{M} represents the number of bits encoded into each QAM symbol. The BER is then approximated by [40]

$$\text{BER} \approx \frac{(1 - L^{-1})}{\log_2 L} \text{erfc}\left[\sqrt{\frac{3\log_2 L}{(L^2 - 1)} \frac{\sqrt{2}}{(k\text{EVM})^2 \log_2 M}}\right].$$

Fig. 8 illustrates the measured EVM of QPSK with rectangular points and 16-QAM by triangular points. As can be seen from this figure, the QPSK signal could travel almost 120 m with its EVM reaching 25% although a 16-QAM signal could only travel up to 40 m successfully. According to the presented measurements, the proposed system of an RF signal generator based on optical solitonic input with a minimum input power of 10 dBm is applicable for a 50 km optical link and a maximum of 120 m wireless distance with QPSK modulation. The constellation diagram for 16-QAM and QPSK signals transmission are presented in Fig. 9. Based on Fig. 9, in this study, the acceptable wireless distances for 16-QAM and QPSK signals are 40 and 120 m, respectively. Therefore, this system can support a maximum wireless transmission distance of 120 m.

5. Conclusion

This paper has described a proposal and successful demonstration of a ring laser system to generate soliton pulses. This ring laser system was first used to generate a soliton with

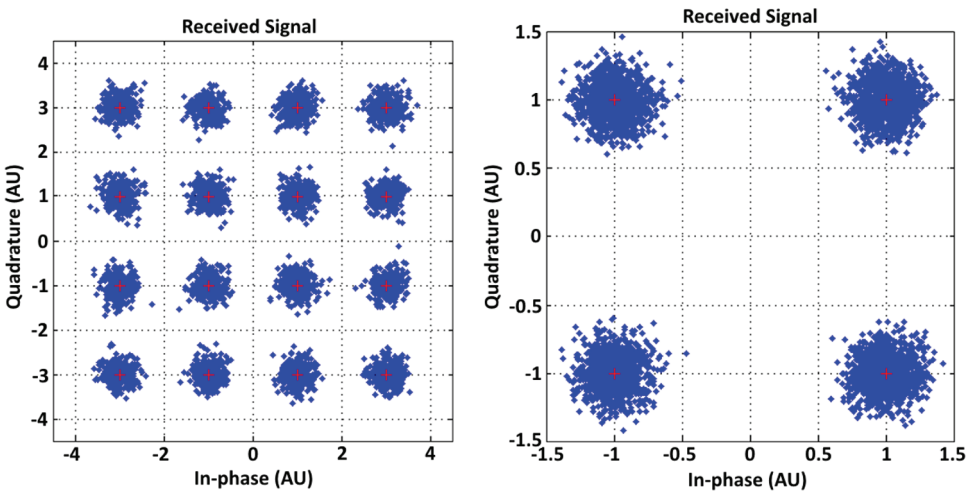

Fig. 9. Constellation measurement of 16-QAM (for 40m wireless distant) and QPSK (for 120 m wireless distance).

differently centered wavelengths, in which a bright soliton was passed through a 50 km SMF and impacted on a PIN photodetector at the other end. Consequently RF arrays were generated in the range of WiFi frequencies. A carrier centered in the 2.5 GHz band was selected for modulation via QPSK and 16-QAM. The RF spectrum was analyzed following propagation along a 250 m wireless link, and the power variations were measured. Measurements confirmed that the proposed system of RF signal generation based on optical solitonic input with the minimum input power of 10 dBm could be used for 50 km optical link and a maximum of 120 m wireless distance with QPSK data signal. The authors anticipate the work presented here will form a basis for further studies in this area. Future work intended to simplify the generation of mode-locked signals may result in significant gains if the approach involves a focus on simplifying integration aspects within the photonics domain.

Acknowledgement

The authors would like to thank the administration of Universiti Teknologi Malaysia for providing research facilities and support.

References

[1] X. S. Yao and G. Lutes, "A high-speed photonic clock and carrier recovery device," *IEEE Photon. Technol. Lett.*, vol. 8, no. 5, pp. 688–690, May 1996.
[2] L. Huo, Y. Dong, C. Lou, and Y. Gao, "Clock extraction using an optoelectronic oscillator from high-speed NRZ signal and NRZ-to-RZ format transformation," *IEEE Photon. Technol. Lett.*, vol. 15, no. 7, pp. 981–983, Jul. 2003.
[3] Y.-C. Chi and G.-R. Lin, "A self-started laser diode pulsation based synthesizer-free optical return-to-zero on-off-keying data generator," *IEEE Trans. Microw. Theory Techn.*, vol. 58, no. 8, pp. 2292–2298, Aug. 2010.
[4] S. E. Alavi, I. S. Amiri, H. Ahmad, A. S. M. Supa'at, and N. Fisal, "Generation and transmission of 3 × 3 W-band MIMO-OFDM-RoF signals using micro-ring resonators," *Appl. Opt.*, vol. 53, no. 34, pp. 8049–8054, 2014.
[5] I. S. Amiri and J. Ali, "Data signal processing via a Manchester coding-decoding method using chaotic signals generated by a PANDA ring resonator," *Chin. Opt. Lett.*, vol. 11, no. 4, Apr. 2013, Art. ID. 041901.
[6] I. S. Amiri, S. E. Alavi, S. M. Idrus, A. Nikoukar, and J. Ali, "IEEE 802.15.3c WPAN standard using millimeter optical soliton pulse generated by a panda ring resonator," *IEEE Photon. J.*, vol. 5, no. 5, Oct. 2013, Art. ID. 7901912.
[7] I. S. Amiri, S. E. Alavi, N. Fisal, A. S. M. Supa'at, and H. Ahmad, "All-optical generation of two IEEE802.11n signals for 2 × 2 MIMO-RoF via MRR system," *IEEE Photon. J.*, vol. 6, no. 6, Dec. 2014, Art. ID. 7903611.
[8] S. E. Alavi *et al.*, "W-band OFDM for radio-over-fibre direct-detection link enabled by frequency nonupling optical up-conversion," *IEEE Photon. J.* vol. 6, no. 6, Dec. 2014, Art. ID. 7903908.
[9] S. E. Alavi *et al.*, "All optical OFDM generation for IEEE802.11a based on soliton carriers using microring resonators," *IEEE Photon. J.*, vol. 6, no. 1, Feb. 2014, Art. ID. 7900109.
[10] I. S. Amiri, A. Nikoukar, and J. Ali, "GHz frequency band soliton generation using integrated ring resonator for WiMAX optical communication," *Opt. Quantum Electron.*, vol. 46, no. 9, pp. 1165–1177, Sep. 2013.

[11] I. S. Amiri, S. E. Alavi, H. Ahmad, A. S. M. Supa'at, and N. Fisal, "Numerical computation of solitonic pulse generation for terabit/sec data transmission," *Opt. Quantum Electron.*, Oct. 2014, DOI:10.1007/s11082-014-0034-9.
[12] I. S. Amiri, M. R. K. Soltanian, S. E. Alavi, and H. Ahmad, "Multi wavelength mode-lock soliton generation using fiber laser loop coupled to an add-drop ring resonator," *Opt. Quantum Electron.*, Jan. 2015, DOI:10.1007/s11082-015-0125-2.
[13] I. S. Amiri, A. Afroozeh, and H. Ahmad, *Integrated Micro-Ring Photonics: Principles and Applications as Slow Light Devices, Soliton Generation and Optical Transmission*. New York, NY, USA: Taylor & Francis, 2015.
[14] I. S. Amiri and A. Afroozeh, *Ring Resonator Systems to Perform Optical Communication Enhancement Using Soliton*. New York, NY, USA: Springer-Verlag, 2014.
[15] N. Madamopoulos *et al.*, "Applications of large-scale optical 3D-MEMS switches in fiber-based broadband-access networks," *Photon. Netw. Commun.*, vol. 19, no. 1, pp. 62–73, Feb. 2010.
[16] E. Wong, "Next-generation broadband access networks and technologies," *J. Lightw. Technol.*, vol. 30, no. 4, pp. 597–608, Feb. 2012.
[17] J. Chung, Y. Yun, and S. Choi, "Prototype implementation of adaptive beamforming–MIMO OFDMA system based on IEEE 802.16e WMAN standard and its experimental results," *Int. J. Commun. Syst.*, vol. 24, no. 12, pp. 1627–1646, Dec. 2011.
[18] J. D. Chen, F. B. Ueng, and P. F. Lin, "A low-complexity adaptive receiver for DS-CDMA systems in unknown code delay environment," *Int. J. Commun. Syst.*, vol. 24, no. 2, pp. 225–238, Feb. 2011.
[19] S. Hranilovic, "On the design of bandwidth efficient signalling for indoor wireless optical channels," *Int. J. Commun. Syst.*, vol. 18, no. 3, pp. 205–228, Apr. 2005.
[20] J. S. Leu and S. F. Chen, "TRASS: A transmission rate-adapted streaming server in a wireless environment," *Int. J. Commun. Syst.*, vol. 24, no. 7, pp. 852–871, Jul. 2011.
[21] M. S. Sharawi and D. N. Aloi, "Characterizing the performance of single-channel pseudo-Doppler direction finding systems at 915 MHz for vehicle localization," *Int. J. Commun. Syst.*, vol. 24, no. 1, pp. 27–39, Jan. 2011.
[22] F. Kartner, I. Jung, and U. Keller, "Soliton mode-locking with saturable absorbers," *IEEE J. Sel. Topics Quantum Electron.*, vol. 2, no. 3, pp. 540–556, Sep. 1996.
[23] F. Kurtner, J. A. der Au, and U. Keller, "Mode-locking with slow and fast saturable absorbers-what's the difference?" *IEEE J. Sel. Topics Quantum Electron.*, vol. 4, no. 2, pp. 159–168, Mar./Apr. 1998.
[24] I. S. Amiri *et al.*, "Transmission of data with orthogonal frequency division multiplexing technique for communication networks using GHz frequency band soliton carrier," *IET Commun.*, vol. 8, no. 8, pp. 1364–1373, May 2014.
[25] I. S. Amiri *et al.*, "W-band OFDM transmission for radio-over-fiber link using solitonic millimeter wave generated by MRR," *IEEE J. Quantum Electron.*, vol. 50, no. 8, pp. 622–628, Aug. 2014.
[26] Y.-H. Lin, J.-Y. Lo, W.-H. Tseng, C.-I. Wu, and G.-R. Lin, "Self-amplitude and self-phase modulation of the charcoal mode-locked erbium-doped fiber lasers," *Opt. Exp.*, vol. 21, no. 21, pp. 25184–25196, Oct. 2013.
[27] Y.-H. Lin *et al.*, "Soliton compression of the erbium-doped fiber laser weakly started mode-locking by nanoscale p-type Bi2Te3 topological insulator particles," *Laser Phys. Lett.*, vol. 11, no. 5, May 2014, Art. ID. 055107.
[28] I. Amiri, J. Ali, and P. Yupapin, "Enhancement of FSR and finesse using add/drop filter and PANDA ring resonator systems," *Int. J. Modern Phys. B*, vol. 26, no. 4, Feb. 2012, Art. ID. 1250034.
[29] I. S. Amiri and J. Ali, "Optical quantum generation and transmission of 57–61 GHz frequency band using an optical fiber optics," *J. CTN*, vol. 11, pp. 2130–2135, 2014.
[30] L. Kong, X. Xiao, and C. Yang, "Operating regime analysis of a mode-locking fiber laser using a difference equation model," *J. Opt.*, vol. 13, no. 10, Oct. 2011, Art. ID. 105201.
[31] G. Agrawal, *Applications of Nonlinear Fiber Optics*. New York, NY, USA: Academic, 2010.
[32] R. Weill, A. Bekker, V. Smulakovsky, B. Fischer, and O. Gat, "Spectral sidebands and multipulse formation in passively mode-locked lasers," *Phys. Rev. A*, vol. 83, Apr. 2011, Art. ID. 043831.
[33] W. Chang, J. Soto-Crespo, A. Ankiewicz, and N. Akhmediev, "Dissipative soliton resonances in the anomalous dispersion regime," *Phys. Rev. A*, vol. 79, Mar. 2009, Art. ID. 033840.
[34] J. Soto-Crespo, M. Grapinet, P. Grelu, and N. Akhmediev, "Bifurcations and multiple-period soliton pulsations in a passively mode-locked fiber laser," *Phys. Rev. E*, vol. 70, 2004, Art. ID. 066612.
[35] D. Tang, L. Zhao, B. Zhao, and A. Liu, "Mechanism of multisoliton formation and soliton energy quantization in passively mode-locked fiber lasers," *Phys. Rev. A*, vol. 72, 2005, Art. ID. 043816.
[36] X. Liu, "Dynamic evolution of temporal dissipative-soliton molecules in large normal path-averaged dispersion fiber lasers," *Phys. Rev. A*, vol. 82, Dec. 2010, Art. ID. 063834.
[37] G. P. Agrawal, *Nonlinear Fiber Optics*. New York, NY, USA: Academic, 2007.
[38] X. Liu, "Hysteresis phenomena and multipulse formation of a dissipative system in a passively mode-locked fiber laser," *Phys. Rev. A*, vol. 81, Feb. 2010, Art. ID. 023811.
[39] G. Martel *et al.*, "On the possibility of observing bound soliton pairs in a wave-breaking-free mode-locked fiber laser," *Opt. Lett.*, vol. 32, no. 4, pp. 343–345, Feb. 2007.
[40] R. Schmogrow *et al.*, "Error vector magnitude as a performance measure for advanced modulation formats," *IEEE Photon. Technol. Lett.*, vol. 24, no. 1, pp. 61–63, Jan. 2012.